

Manuscript Title: with Forced Linebreak

Alon Shaaltiel and Oren Kereth
*Raymond and Beverly Sackler School of Physics and Astronomy,
 Faculty of Exact Sciences, Tel Aviv University, Tel Aviv 69978, Israel*
 (Dated: December 19, 2021)

An article usually includes an abstract, a concise summary of the work covered at length in the main body of the article.

Usage: Secondary publications and information retrieval purposes.

Structure: You may use the `description` environment to structure your abstract; use the optional argument of the `\item` command to give the category of each item.

1. INTRODUCTION

In this experiment the Fourier Transform Infra Red spectrometer (FTIR) will be used extensively to extract the IR spectra of various materials and compounds. Let us start with a short historical review. In 1800 IR was recognized as a distinct region of the energy spectrum by Sir William Herschel, however the study of IR light with various materials started about 100 years later. In 1903, William W. Coblentz measured the IR spectra of hundreds of inorganic and organic compounds. As a result of increasing interest in the field, the first prototypes of IR spectroscopy were built in the 1930s. In 1949 the astrophysicist Peter Fellgett used an interferometer to measure light from celestial bodies and produced the first Fourier transform infrared spectrum, however this method was still limited and took many hours to compute. In the late 1960s commercial FTIR spectrometers appeared because microcomputers were able to do the Fourier transform, however they were large and expensive. Over time, technology reduced the costs, increased availability and enhanced the capabilities of FTIR spectroscopy systems[1]

1.1. Thin Film Interference

Upon contact with a beam of light, the internal reflections in a thin sample of material with a sufficiently low refractive index are not negligible.

This experiment concerns only the transmitted beams; The reflected beams are quite similar. The phase between two consecutive transmitted beams and relative intensity are

$$\Delta\varphi = 2n_2 d \cos(\theta); \frac{I_{n+1}}{I_n} = r^2 \quad (1)$$

where r is the reflection coefficient of the material and is smaller than 1, d is the sample's thickness, θ is the beam's angle inside the sample, n_2 is the sample's refractive index and I_n is the n -th transmitted beam's intensity. Constructive interference occurs if $\Delta\varphi = \frac{m}{k}$ and

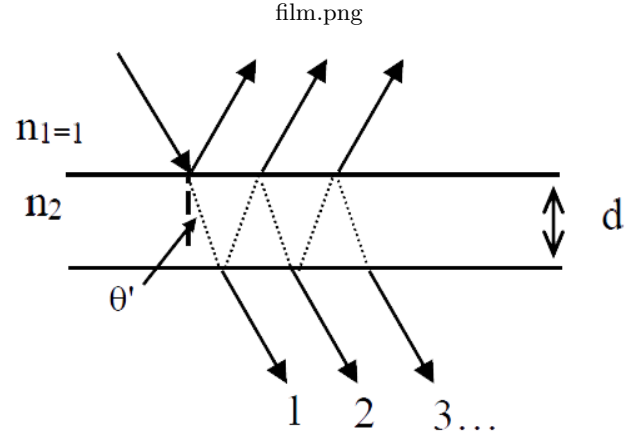


FIG. 1.1. Reflected and transmitted light waves from a thin film

if $\Delta\varphi = \frac{m+\frac{1}{2}}{k}$, destructive interference occurs. The difference in k , the wavenumber, between two constructive peaks is

$$\Delta k = \frac{1}{2n_2 d \cos(\theta)} \quad (2)$$

The transmitted intensity $I_{tot} = \sum I_i$ is proportional to $\sin(\frac{1}{\Delta k} k) + const.$

1.2. The Beer-Lambert Law

The Beer-Lambert Law describes how a monochromatic beam of light is absorbed in relation to substance concentration. The dependency is given by

$$\ln\left(\frac{P(v)}{P_0(v)}\right) = A = -av_{\alpha\alpha'} C x \quad (3)$$

where $P(v)$ is the light's intensity through the sample, $P_0(v)$ is the intensity with no sample, A is the absorbance, a is the molar attenuation coefficient, α and α' are quantum numbers, C is the concentration, and x is the optical path length of the beam. All else being

equal, the absorbance and concentration are proportional to one another.

1.3. CO Molecule IR Spectrum

The model used to describe this molecule and other diatomic molecules pictures a molecule in which the individual atoms, held together by chemical bonds, are in vibratory motion along these bonds, while the molecule as a whole is rotating [2]. The energy states of this system correspond to a Hamiltonian with a potential

$$V(\mathbf{r}) = \frac{1}{2}k(r - r_0)^2 \quad (4)$$

and can be expressed as a combination of rotational and vibrational energies

$$E = E_{Rot} + E_{Vib} = hcw_e(\nu + \frac{1}{2}) + \frac{\hbar^2}{2I}J(J+1) \quad (5)$$

where h is Planck's constant, c is the speed of light, w_e is the wave number corresponding to the frequency of vibrations, ν is a quantum number corresponding to the vibrations, I is the molecule's moment of inertia and J is a quantum number corresponding to the angular momentum of the particle [3]. However, the potential is not truly harmonic, as effects such as the centrifugal force, Coriolis and Fermi [2] require the use of perturbation theory [4]. Using the perturbation theory, the energy states are now

$$\begin{aligned} T &= T_{Vib} + T_{Rot} = \\ &w_e(\nu + \frac{1}{2}) - w_ex_e(\nu + \frac{1}{2})^2 + \\ &B_vJ(J+1) - D_vJ^2(J+1)^2 \end{aligned} \quad (6)$$

where x_e , B_v and D_v are constants which take into account small perturbations and T is the energy states in wave number units ($T = \frac{E}{hc}$). At room temperature only the $\nu = 0$ state is occupied while the J states are all occupied. Therefore, using selection rules [3] only the transitions $\nu \rightarrow \nu'$ where $\nu' = 1, 2, 3$ and $J \rightarrow J'$ where $J' = J+1, J-1$ are of interest. Using equation (need to add reference for the right equation) the allowed spectral lines are derived to be

$$\begin{aligned} \Delta T &= T(\nu', J') - T(\nu, J) = \\ &w_e\nu' - w_ex_e(\nu'^2 + \nu'^2) + (2B_e - \alpha(\nu' + 1))m - \\ &\alpha\nu'm^2 - 4D_v m^3 \end{aligned} \quad (7)$$

where ΔT is the allowed spectral line, B_e, α are constants related to B_v which are the result of further corrections due to perturbation theory and m is either $J+1$ or $J-1$ depending on the transition. In this experiment only the transition to $\nu' = 1$ will be of interest, for which $\Delta T = 2141 \frac{1}{cm}$ (maybe put a reference, maybe it's in STUART)

2. EXPERIMENTAL SYSTEM AND MEASUREMENTS

There are two main measuring instruments in this experiment- FTIR and ATR. Both use Michelson interferometers and perform a Fourier transform.

2.1. Michelson Interferometers

A Michelson interferometer consists of two perpendicularly plane mirrors, one of which can travel in a direction perpendicular to the plane. A semi reflecting film, the beamsplitter, bisects the planes of these two mirrors. The beamsplitter splits the beam into two, one beam transmitted through the beamsplitter and the other reflected from it. Both beams then get reflected from the mirrors, returning to the beamsplitter where they recombine and interfere [5] (see Figure 2). The beam which emerges

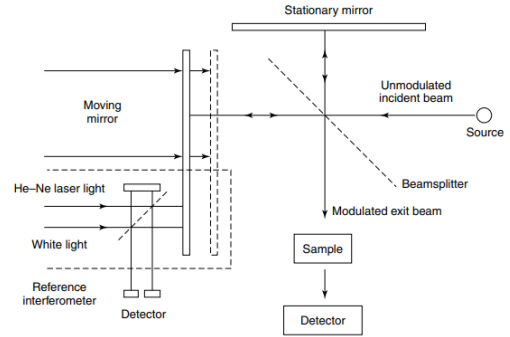


FIG. 2.2. Schematic of a Michelson interferometer [5].

from the interferometer at 90 degrees to the input beam is called the transmitted beam and is the beam detected by the detector. The moving mirror produces an optical path difference between the two beams split by the beamsplitter. Plotting the signal produced as a function of the change of pathlength between the two beams will yield an interferogram. By performing a Fourier transform on the interferogram the spectral distribution of the beam (i.e. the amplitude of each wave number the light is consisted of) can be found.

2.2. FTIR

FTIR stands for Fourier transform infrared. IR radiation is passed through a sample. Some of the infrared radiation is absorbed by the sample and some of it is passed through (transmitted). The resulting spectrum represents the molecular absorption and transmission [6]. FTIR (see Figure 3) utilises Michelson interferometers, the interferogram and a Fourier transform to perform the analysis of the spectrum.

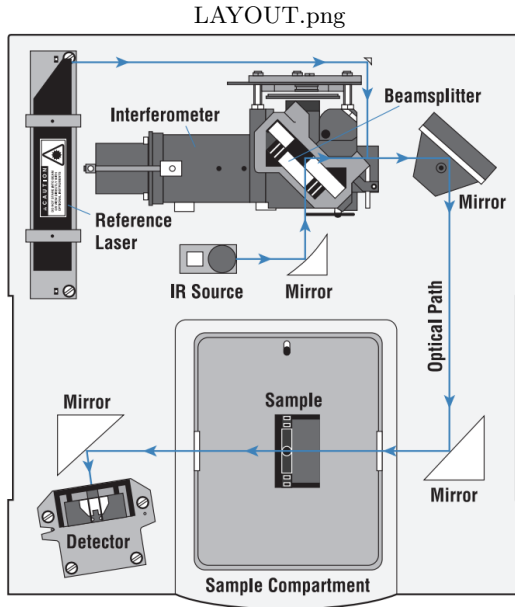


FIG. 2.3. Layout of the FTIR spectrometer [6].

The main components of the FTIR spectrometer are the source, a black-body source from which the IR radiation is emitted. The radiation then passes through an interferometer, where the 'spacial encoding' takes place [6]. A He-Ne laser is used as a reference for calibration of the moving mirror's position [5]. After going through the interferometer, an interferogram is created. The interferogram then passes through the sample, where specific wave numbers are absorbed according to the sample's characteristics and the rest are transmitted into the detector where the interferogram signal is measured. The data reaches the computer, which performs a Fourier transform yielding the infrared spectrum consisting of absorption lines corresponding to the sample.

2.3. ATR

ATR, which stands for Attenuated Total Reflection, measures the absorbance of a liquid or solid using IR spectroscopy. A crystal with a sufficiently high refractive index to achieve total internal reflection is surrounded by the material whose absorbance is measured. An interfer-

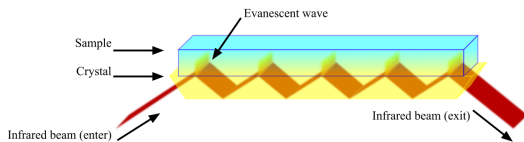


FIG. 2.4. Layout of an ATR compartment [7]

ogram is projected into the crystal and evanescent waves, resulting from the total internal reflection, propagate

through the sample. In a vacuum, the energy evanescent waves carry is wholly returned. However, when a sample is inserted, wavelengths corresponding with the sample's normal modes are absorbed. As other wavelengths are not affected, the loss in intensity across the interferogram is very small when compared with a projection through the sample. As described in the previous paragraph, the interferogram is detected and disassembled into the sample's infrared spectrum.

2.4. Transmission Through Thin Films of Polyester

In this part of the experiment the refractive index of a thin sample of Polyester is extracted. Thin Polyester samples with varying widths are placed in the sample area perpendicular to the beam's direction. An interferogram is projected through each sample. The resulting IR spectrum will include both the absorbance spectrum of the Polyester and the sine wave of thin film interference. To extract the frequency of interference an area of low absorbance in the spectrum is sought out, and a sine wave is fitted. Using equation 2, the extracted sine frequency, the measured width and under the assumption that $\theta = \frac{\pi}{2}$ a fit of the form

$$d = a_0 + a_1 f_{fit} \quad (8)$$

was made. Where d is the sample width, f_{fit} is the frequency of the fitted sine with a theoretical value of $\frac{1}{\Delta k}$, a_1 is the slope with a theoretical value of $2n_2$ and a_0 is the constant with a theoretical value of 0. Using the relation between the fitted frequency and width, the widths of three samples were found.

2.5. Calibration Using Ethanol

In this part of the experiment the relationship between the concentration of a dissolved substance inside a solution to its total absorbance amplitude, which is assumed to be linear according to equation 3 was calibrated. The calibration was done using mixtures of water and ethanol with varying known concentrations. The mixture was put into a tank inside an ATR. Starting from a concentration of 96% , the ethanol was diluted by adding more water into the mixture, thus changing the concentration of the ethanol according to

$$C_i V_i = C_f V_f \quad (9)$$

where C_i, V_i, C_f, V_f are the initial and final concentration of ethanol and volume of the mixture respectively. For each concentration, F , the total absorbance of ethanol in the range $1000 - 1120 \frac{1}{cm}$ was calculated and a calibration graph of the form

$$C = a_0 + a_1 F \quad (10)$$

was made. Where C is the concentration of ethanol in the mixture. Using the calibration, the concentration of different solutions was found.

2.6. CO₂ and IR Spectrum of CO

Using a pump, exhaled and outside air were each inserted into a chamber in the FTIR. For each of the two types of air the total absorbance in the IR spectrum in the range $2270 - 2400 \frac{1}{cm}$ were calculated. In this region there are two absorption peaks both corresponding to the concentration of CO₂ in the air. The ratio between the total absorbance of the exhaled air to the outside air in that region, denoted by S is therefore equal to the corresponding ratio between CO₂ concentrations in each of them. S will then be compared to ratios previously measured. Afterwards, by pumping CO into to the same chamber in the FTIR and its IR spectrum was measured. According to equation 8, the spectrum contains absorption peaks that represent a transition in the angular momentum of the molecule, J to either $J + 1$ or $J - 1$ (see Figure 5) Each of the peaks, m , were numbered according to its

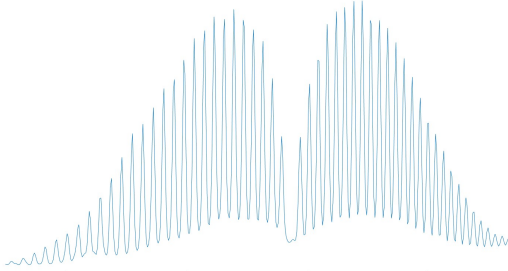


FIG. 2.5. CO absorption lines in the region $2025 - 2033 \frac{1}{cm}$. Each peak represents a transition m of the angular momentum and the transition from $\nu = 0$ to $\nu' = 1$ which is centered at $2142 \frac{1}{cm}$ as can be seen and according to subsection 1.3.

order relative to the center point at $2142 \frac{1}{cm}$ (i.e. if m was the first to its left it was numbered as -1 and if it was the first to its right it was numbered as 1). Afterwards, a polynomial fit of 3^{rd} order was made between ΔT from equation 8 and m

$$\Delta T = a_0 + a_1 m + a_2 m^2 + a_3 m^3 \quad (11)$$

The coefficients extracted from the fit will then be used to extract the coefficients in equation 8 according to the relations

$$\alpha = -a_2 \quad D_v = -\frac{a_3}{4} \quad w_e = 2a_0 - \frac{4255}{2}$$

$$B_e = \frac{a_1 - 2a_2}{2} \quad x_e = \frac{a_0 - \frac{4255}{2}}{2a_0 - \frac{4255}{2}}$$

where we used

2.7. IR Spectra of Different Cigarette Brands

In this part of the experiment gasses in the smoke of various cigarettes are analyzed. An interferogram is projected through regular air. A pump smokes on a cigarette and fills the sample area with smoke. An interferogram is projected through the smoke and the absorbance spectrum compared to regular air is created. Various toxic gasses are identified. The gasses' concentrations are estimated using the area of the absorbance peaks.

3. RESULTS

3.1. Ethanol Concentration Calibration

The total absorbance amplitude in the range $1000 - 1120 \frac{1}{cm}$ was calculated numerically for each concentration of ethanol in the mixture using the trapezoidal method[8]. Plotting the IR spectrum of all the mixtures in that range on the same graph (see Figure 6) shows the increasing intensity of the peaks for higher and higher concentrations of ethanol.

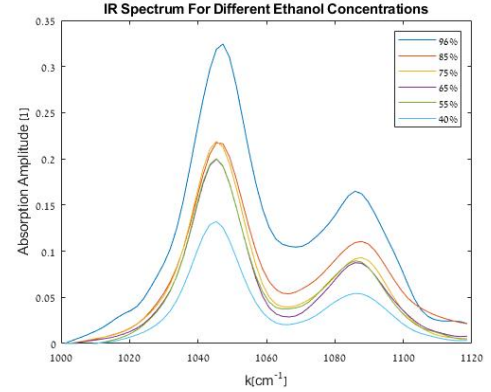


FIG. 3.6. IR spectrum of mixtures with different ethanol concentration in the range $1000 - 1120 \frac{1}{cm}$

Fitting a linear function according to equation 10 to the measurements of concentration and absorbance yielded the following (see Figure 7). The fit parameters extracted from the linear fit can be seen in Table 1 The concentration of ethanol in other mixtures was then

Fit Parameters of Ethanol Calibration Graph		
Parameter	Value	Error (Relative Error)
$a_0[1]$	11.7	9.3(79%)
$a_1[cm]$	7.3	1.4 (19%)

TABLE I. Fit parameters of the ethanol concentration vs absorption amplitude graph

found by numerically calculating the total absorption in

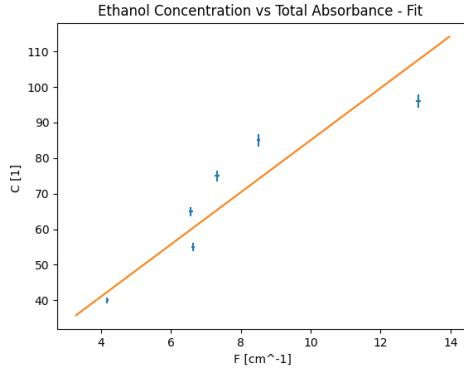


FIG. 3.7. Linear calibration graph of concentration of ethanol in the mixture to total absorbance amplitude in the range $1000 - 1120 \frac{1}{cm}$

the relevant range and plugging it in the linear equation using the fit parameters. Using the fit parameters from Table 1 the concentrations in a Sukutinis and two unknown alcoholic beverages were found (see Table 2).

Ethanol Concentration in Different Beverages			
Beverage	Concentration(%)	Concentration	Error (Relative Error)
Sukutinis	54.3	8.3	(15%)
Unknown 1	40.5	5.7	(14%)
Unknown 2	72	12	(17%)

TABLE II. Ethanol concentration in different beverages

3.2. CO₂

Using the trapezoidal method to calculate the total absorbance of the air in the region $2270 - 2400 \frac{1}{cm}$ which correlates to the concentration of CO₂ (CITE THE WEB-BOOK AGAIN!), the ratio between CO₂ in exhaled air to outside air, S , was calculated yielding

$$S = 61 \quad (12)$$

3.3. CO

The absorption peaks from the IR spectrum of CO were extracted and the absorption lines ΔT and their corresponding angular momentum transitions m were measured relative to the center point at $\Delta T = 2141 \frac{1}{cm}$ which represents $\Delta J = m = 0$ and the vibrational transition from $\nu = 0$ to $\nu' = 1$. Using that data, a 3rd order polynomial fit was made according to equation 11 (see Figure 8). The fit parameters extracted can be seen at Table 3. Using these fit parameters the coefficients at equation 7 were extracted via the relations stated at equation (add ref)

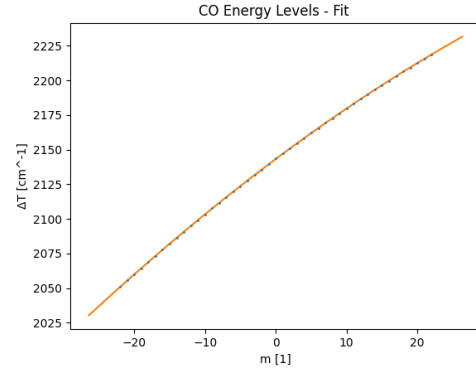


FIG. 3.8. 3rd order polynomial fit of the spectral lines of the absorption peaks ΔT as a function of the transition of the molecule's angular momentum m .

3.4. Polyester Refractive Index Calculation

For each sample width the area with the clearest sine wave in the absorption spectrum was found and fitted to a sine wave. Fitting a linear function between the width

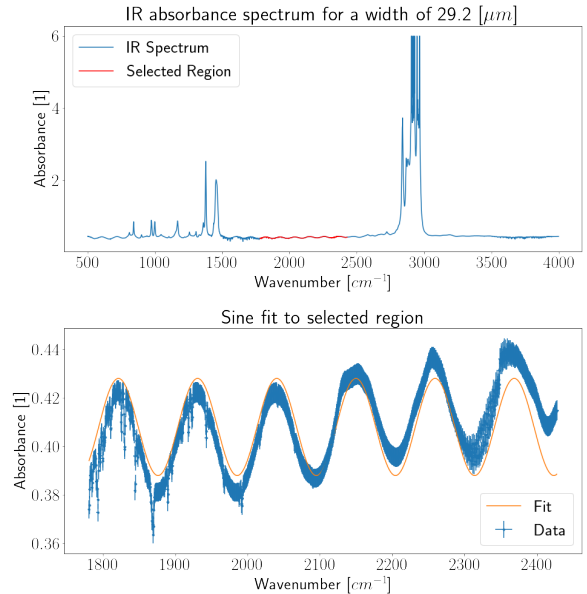


FIG. 3.9. IR absorbance spectrum and sine fit to the selected region for a width of $29.2 \mu m$

and the frequency yielded the following (See Figure 3.3.4) adlak

[1] [www, Ftir instrumentation](http://www.ftir-instrumentation.com) (2008), URL www.

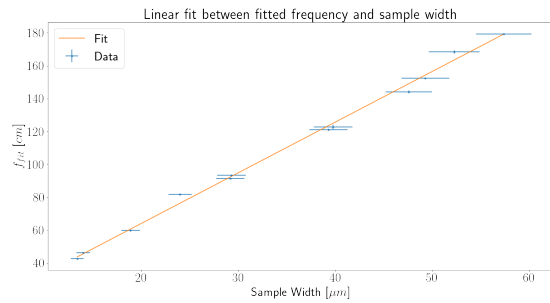


FIG. 3.10. Linear fit between the fitted frequency, f_{fit} , and the sample width.

[2] W. E. K. N. L. Alpert and H. A. Szymanski, *IR Theory and Practice of Infrared Spectroscopy* (Plenum Press New

York, 1970).

- [3] D. J. Griffiths, *Introduction To Quantum Mechanics* (Pearson Education International, 2005).
- [4] J. Sakurai and J. Napolitano, *Modern Quantum Mechanics Second Edition* (Pearson Education International, 2011).
- [5] B. H. Stuart, *Infrared Spectroscopy: Fundamentals and Applications* (John Wiley and Sons, Ltd, 2004).
- [6] *Introduction to Fourier Transform Infrared Spectroscopy*, Thermo Fisher Scientific Inc (2013).
- [7] Attenuated total reflectance, *Attenuated total reflectance — Wikipedia, the free encyclopedia* (2013), [Online; accessed 15-December-2021], URL https://commons.wikimedia.org/wiki/File:ATR_path-en.svg.
- [8] W. T. V. W. H. Press, S. A. Teukolsky and B. P. Flannery, *Numerical Recipes The Art of Scientific Computing Third Edition* (Cambridge University Press, 2007).